REGULATORY INFORMATION DISTRIBUTION SYSTEM (RIDS)

ACCESSION NBR:8201070127 DOC.DATE: 81/12/24 NOTARIZED: NO DOCKET #
FACIL:50-397 WPPSS Nuclear Project, Unit 2, Washington Public Powe 05000397
AUTH.NAME AUTHOR AFFILIATION
BOUCHEY,D.G. Washington Public Power Supply System
RECIP.NAME RECIPIENT AFFILIATION
SCHWENCER,A. Licensing Branch 2

SUBJECT: Forwards responses to Geosciences Branch Questions 360.14 & 360.17.Faults along Rattlesnake-Wallula alignment are not capable according to NRC criteria.Estimates of potential earthquake magnitudes encl.

DISTRIBUTION CODE: B001S COPIES RECEIVED:LTR 1 ENCL 66 SIZE: 40
TITLE: PSAR/FSAR AMDTS and Related Correspondence

NOTES:2 copies all matl:PM. ON Shelf. 05000397

	RECIPIENT ID CODE/NAME		COPIES LTTR	COPIES ENCL	RECIPIENT ID CODE/NAME		COPIES LTTR	COPIES ENCL
ACTION:	A/D LICENSNG		1	0	LIC BR #2 BC		1	0
	LIC BR #2 LA		1	0	AULUCK,R.	01	1	1
INTERNAL:	ELD		1	0	IE	06	3	3
	IE/DEP/EPDB	35	1	1	IE/DEP/EPLB	36	3	3
	MPA		1	0	NRR/DE/CEB	11	1	1
	NRR/DE/EQB	13	3	3	NRR/DE/GB	28	2	2
	NRR/DE/HGEB	30	2	2	NRR/DE/MEB	18	1	1
	NRR/DE/MTEB	17	1	1	NRR/DE/QAB	21	1	1
	NRR/DE/SAB	24	1	1	NRR/DE/SEB	25	1	1
	NRR/DHFS/HFEB	40	1	1	NRR/DHFS/LQB	32	1	1
	NRR/DHFS/OLB	34	1	1	NRR/DHFS/PTRB	20	1	1
	NRR/DSI/AEB	26	1	1	NRR/DSI/ASB	27	1	1
	NRR/DSI/CPB	10	1	1	NRR/DSI/CSB	09	1	1
	NRR/DSI/ETSB	12	1	1	NRR/DSI/ICSB	16	1	1
	NRR/DSI/PSB	19	1	1	NRR/DSI/RAB	22	1	1
	NRR/DSI/RSB	23	1	1	NRR/DST/LGB	33	1	1
	REG FILE	04	1	1				
EXTERNAL:	ACRS	41	16	16	BNL(AMDTS ONLY)		1	1
	FEMA-REP DIV	39	1	1	LPDR	03	1	1
	NRC PDR	02	1	1	NSIC	05	1	1
	NTIS		1	1				

TOTAL NUMBER OF COPIES REQUIRED: LTTR 65 ENCL 60

RR

Washington Public Power Supply System
P.O. Box 968 3000 George Washington Way Richland, Washington 99352 (509) 372-5000

Docket No. 50-397

December 24, 1981
G02-81-551
SS-L-02-CDT-81-113

Mr. A. Schwencer, Director
Licensing Branch No. 2
Division of Licensing
U. S. Nuclear Regulatory Commission
Washington, D.C. 20555

Dear Mr. Schwencer:

Subject: NUCLEAR PROJECT NO. 2
RESPONSES TO REQUESTS FOR INFORMATION

Enclosed are sixty copies of the responses to Geosciences Branch Questions Nos. 360.14 and 360.17. These questions and responses will be incorporated into the next WNP-2 FSAR Amendment.

Even though the response to Question 360.14 concludes that in our best judgement "the faults along RAW are not capable according to USNRC criteria," we have included in the response estimates of potential earthquake magnitudes and resulting ground motion at the site that would be calculated if the faults along RAW were assumed to be capable. These results are consistent with earlier information presented by the Supply System in meetings with the Geosciences Branch and are provided in response to a specific telephone request for the information from the Geosciences Branch.

Very truly yours,

G. D. Bouchey, Deputy Director
Safety and Security

GDB/rch
Enclosures

cc: R Auluck - NRC
WS Chin - BPA
R Feil - NRC
B Jackson - NRC

B001
S1/60 on Shelf

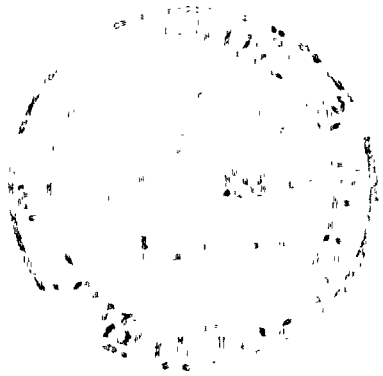

Q. 360.014

Provide your best deterministic judgement of the length, character, and capability of CLEW within the site region. If you determine it to be segmented as reported in the meeting of November 17-18, 1981, provide a map with topographic base delineating the segments and discuss in detail the character and capability of the individual segments, with supporting basis for all judgements.

Response:

The Cle Elum-Wallula lineament (CLEW), as defined by Laubscher (Appendix 2.5-O), is a 240 km-long northwest-trending zone of "en echelon" anticlines that includes part of the Yakima fold belt (Figure 360.014-1). CLEW is coincident with the central third of the Olympic-Wallowa lineament (OWL) which was postulated by Raisz (1945). The portion of CLEW that extends from Rattlesnake Mountain southeastward to the vicinity of Milton-Freewater has been termed the Rattlesnake-Wallula alignment (RAW) (Appendix 2.5K).

As discussed in FSAR Amendment 18, Section 2.5.1.2.5, OWL is not a fundamental crustal boundary of continent-ocean type in the area of the Pasco Basin (Appendix 2.5N). Geologic interpretations (Appendices 2.5Nand 2.5-O) and crustal geophysical studies (Systems, Science, and Software, 1980; Appendix 2.5L) conclude that neither CLEW nor RAW coincide with a major change in crustal composition. Based on the limit of resolution of the north-south trending gravity contours that cross CLEW, the strike-slip displacement parallel to CLEW, if any, cannot be more than 2 to 3 km (Appendix 2.5L); the gravity data do not indicate that strike-slip displacement has occurred. Middle Miocene basalt flows and dikes, and high-angle faults (including the Hite fault) are not displaced by OWL as drawn by Raisz (1945) along the south fork of the Walla Walla River (Kendall, et al, 1981). Therefore, the southeasternmost extent of CLEW is in the area of Milton-Freewater, Oregon.

Tectonic Models

The data do not allow an unequivocal choice between the two prevailing tectonic models: 1) that CLEW is the structural expression of a basement zone of dextral shear that becomes

either deeper (Laubscher, Appendix 2.5-0) or broader and more diffuse (Davis, Appendix 2.5N) to the northwest; or 2) that RAW/CLEW is the consequence of north-south compression of plateau strata against a rigid basement "buttress" having a northwest-trending southern boundary, either with no component of strike-slip deformation or with associated reverse- oblique-slip components (Price, 1981; Woodward-Clyde, 1981). No basement zone of strike-slip faulting is required by the second model. The widespread occurrence of sub-horizontal striae along major faults along RAW (steeply dipping striae are also common) are compatible with either model.

Davis (Appendix 2.5N) defines three structural domains of CLEW (Figure 360.014-1); domains II and III comprise RAW. Domain I extends south from Cle Elem to Rattlesnake Mountain and is defined by a broad zone of deflected or anomalous fold trends. Although Davis included Rattlesnake Mountain in domain I, the Rattlesnake Mountain anticline is similar in structural style and orientation to the doubly-plunging anticlines of domain II. Therefore, the Rattlesnake Mountain anticline has been included in domain II in this analysis.

Laubscher (Appendix 2.5-0) proposes that the broad deformation of domain I is the result of a transcurrent structure at depths of 15 to 20 km. An alternative explanation for the features of domain I is not that the controlling structure is deeper, but that the zone of "basement" wrenching is broader and more diffuse to the northwest of Rattlesnake Mountain (Davis, 1981).

In neither Laubscher's or Davis' model is a throughgoing fault proposed in domain I that may be potential seismic source. No evidence of throughgoing faults is present at the surface within domain I. A transcurrent structure at depths of 15 to 20 km, as proposed by Laubscher, would be at or near the maximum depth of seismicity in the Columbia Plateau and would lie within the lowermost crust and/or the upper mantle. Davis (1981) postulates a broad diffuse zone of deformation beneath the folds of domain I; this also argues against a throughgoing structure at depth. Therefore, the discussion of potential seismic sources, capability, and maximum magnitudes is based on an analysis of the RAW portion of CLEW (i.e., domains II and III).

The following discussions of segmentation, capability, maximum magnitudes, and ground motions are presented for both tectonic models: strike-slip faulting; and reverse-oblique-slip faulting.

Capability

The weight of the available geologic and seismologic evidence leads us to conclude that the faults along RAW are not capable according to the USNRC criteria.

There is no historical or instrumental seismicity associated with any of the faults along RAW and there is no geologic evidence that indicates there has been any single displacement during the past 35,000 years or multiple displacements during the past 500,000 years. Only indirect evidence might suggest that the faulting along RAW could be capable. The instrumental seismicity data for the Columbia Plateau shows that the region is undergoing north-south compression. The presence of relatively young scarps that are apparently fault related along Toppenish Ridge, and the displaced Pleistocene (?) gravels at Union Gap suggest that deformation due to north-south compression may still be occurring locally within the plateau. The orientation of RAW with respect to the present stress field, is compatible with either reverse-oblique-slip, or with right-lateral strike-slip.

The assessment of the capability of individual faults along the RAW trend is, in part, dependent upon the style of deformation (tectonic model) that is attributed to RAW. If RAW is characterized by strike-slip faulting, all the parts of the structure are likely to exhibit the same capability (i.e., either capable or not capable); whereas, if RAW is characterized by reverse-oblique faulting, the different fault segments may exhibit different capability.

The available geologic evidence regarding the age of the most recent displacement on faults along RAW is summarized below.

Wallula Gap Fault - At Warm Springs Canyon, colluvial deposits that post-date the Columbia River basalt but pre-date the late Pleistocene flood deposits are in fault contact with the Frenchman Springs Member of the Saddle Mountains Formation (Miocene). The age of the faulted colluvial deposits is uncertain. They could be as old as the Ringold Formation (Miocene - Pliocene), but they are probably early to middle Pleistocene in age. At Warm Springs Canyon, the late Pleistocene Touchet deposits (13,000 years B.P.) overlie the Wallula Gap fault and are not displaced. At Yellepit, the Wallula Gap fault is overlain by deposits of the Kennewick fanglomerate, which are not displaced. The Kennewick fanglomerate pre-dates a caliche soil horizon that is greater than 20,000 years old.

Finley Quarry - A 13 m-wide zone containing 3 fault traces was exposed in a trench in Finley Quarry at the northeast end of the Butte. The northern and central fault traces displace colluvial deposits that post-date the Columbia River Basalt. These faulted deposits are overlain by unfaulted colluvium. At the northern end of the exposure, this unfaulted unit is overlain by two caliche soil horizons. Uranium-thorium dates on caliche rinds indicate that the upper soil is at least 70,000 years old. Presumably the lower caliche, which is thicker, is much older; conceivably, it is equivalent in age to pre-Quaternary soils developed on fanglomerates that grade to the Ringold Formation in the Pasco Basin. Minimum ages for the soils can be estimated based on correlation to intervals of climatic warming interpreted from deep sea cores (Shackleton and Opdyke, 1973). The degree of soil profile development (stage II to III carbonate development) and the minimum age of 70,000 years B.P. suggest that the upper paleosol formed during the Sangamon Interglacial (oxygen isotope stage 5), which lasted from about 125,000 to 75,000 B.P. By inference, the lower paleosol may have formed during oxygen isotope stage 7, which lasted from 251,000 to 195,000 years B.P.

Rattlesnake Mountain Fault - There is no evidence that indicates there has been any Quaternary displacement on the Rattlesnake Mountain fault. However, no Quaternary deposits have been mapped along this structure that are of sufficient age to prove that the fault is not capable. Late Pleistocene and Holocene landslide deposits and eolian deposits overlie the fault and are not displaced.

The absence of any historical or instrumental seismicity associated with faults along RAW and the absence of any geologic evidence for recent displacement suggests that the faults along RAW are not capable. There is geologic evidence that indicates there has been no displacement on the Wallula Gap fault, which occurs along the southeastern domain of RAW, during at least the past 20,000 years. There is geologic evidence at Finley Quarry that suggests there has been no displacement on the structural domain extending from near Wallula Gap to Rattlesnake Mountain during at least the past 70,000 years and probably not within about the past 200,000 years. The data do not preclude the possibility of the faults having very long recurrence intervals (hundreds of thousands of years). However, the weight of the available geologic and seismologic evidence leads us to conclude that the faults along RAW are not capable according to the USNRC criteria.

The following discussions on segmentation, maximum earthquake magnitudes and ground motions are presented to indicate the significance of RAW to the SSE if it were assumed that faults along RAW are capable.

Segmentation

Geologic and geomorphic data may be used to define the parts of a fault that represent earthquake rupture segments or structural domains that exhibit uniform behavior through time. Geologic relationships reflect the past history of deformation along a structure in terms of fault location fold/fault relationships, and style of deformation. Therefore, a knowledge of the history of deformation can allow estimates of the future behavior of faults.

Domains II and III along RAW are defined because they exhibit similar styles of deformation through geologic time. In the vicinity of Wallula Gap, RAW exhibits a pronounced change in structural style that reflects a segmentation of the zone (Figure 360.014-1). Structural domain III to the southeast is defined by a complex zone of folding and apparent strike slip to reverse oblique-slip faulting along the Wallula Gap fault. Domain II to the northwest is defined by an alignment of structural domes, doubly-plunging anticlines, and relatively minor faults. Detailed mapping along domain II of RAW has shown that faults are discontinuous and are apparently limited to individual domes. These domains do not represent fault rupture segments.

The lengths of fault-rupture segments are estimated based on evidence of segmentation, dimensions of known faults, and an understanding of tectonic models. Because of differences in the mechanics of rupture, there appears to be a higher probability that surface geologic and geomorphic relationships define the segmentation of dip-slip faults than they do for strike-slip faults. For this reason, RAW is segmented somewhat differently for a strike-slip tectonic model than for a reverse-oblique-slip model.

Reverse-Oblique-Slip Model:

For a reverse-oblique-slip model, it is assumed that future fault behavior will be consistent with past behavior estimated from geologic evicence. In domain II, fault rupture segments will most likely coincide with known faults and rupture dimensions will be limited by fold dimensions. The longest known fault along this domain and the closest fault

to the site is the Rattlesnake Mountain fault. In domain III, the Wallula Gap fault zone is the longest fault that could be a potential seismic source.

Strike-Slip Model:

Although the structural domains of RAW probably apply to all tectonic models, it is possible that surface geologic and geomorphological relationships may not define the segmentation of strike-slip faults having little or no verticle component of slip. There is no evidence for a throughgoing strike-slip fault in domain II. However, if this evidence is disregarded, there is little basis for segmenting RAW if one assumes a strike-slip model. Therefore, fault parameters for a strike-slip model are developed assuming RAW is not segmented.

Fault Parameters

Reverse-Oblique-Slip:

As discussed previously, the faults having potential significance to the site, if they are seismogenic sources, are the Wallula Gap fault and the Rattlesnake Mountain fault. The Wallula Gap fault has a maximum inferred length of 45 km. Assuming that up to half of the total fault length may rupture during an earthquake, the maximum rupture length for the Wallula Gap fault is 23 km. The Rattlesnake Mountain fault has a mapped length of 7 km and, assuming it connects with the short fault that is mapped on strike to the northwest (FSAR Section 2.5.1.2.4.4.1), it has an inferred length of 10 km. The maximum length of the fault is estimated to be 20 km by assuming that the fault extends southward along the entire length of the Rattlesnake Mountain anticline. Rupture lengths of 5 km and 10 km are estimated based on assumed half-length rupture.

The downdip fault widths of both the Wallula Gap fault and the Rattlesnake Mountain fault are uncertain but may be estimated from crustal models that are based on seismicity and geophysical data (Appendix 2.5K). The estimates of fault width are based on dipping fault surfaces and range from 5 to 11 kilometers. The 5 km width is derived using a fault that dips 60 degrees and extends to a depth of 4 km; the 4 km depth is the maximum depth to the base of the Columbia River basalts based on gravity data (Appendix 2.5L). A width of 11 km is obtained using the average maximum depth to basement based on a time-term analysis (Eaton, 1976) of 7.5 km and a fault dip of 45 degrees.

The following table summarizes the magnitude-related fault parameters for the Wallula fault and the Rattlesnake Mountain fault assuming a reverse-oblique model:

	Wallula Fault	Rattlesnake Mountain Fault
Total Length	45 km	10 to 20 km
Rupture Length	23 km	5 to 10 km
Fault Width	5 to 11 km	5 to 11 km

Strike-Slip Model:

Assuming RAW is not segmented, the rupture length may be estimated in two ways: 1) by assuming that a percentage of the total structure length will rupture, and 2) by assuming that the rupture length will be one-half of the longest mapped fault. To estimate the percentage rupture, the relationship of Slemmons (1980; pers. comm., 1981) developed for strike-slip faults may be used:

$$P_{RL} = 11.7 + 0.016\ (L_T)$$

where L_T is the total fault length in kilometers and P_{RL} is the percentage of total rupture length. The total lengths used in Slemmons' (1980) relationship are the maximum lengths of strike-slip fault systems. To apply the relationship to RAW, it is assumed that the more continuous faulting observed in domain III extends to the northwest into domain II as well. As discussed previously, the data do not suggest a continuous fault zone along domain II. Based on a total assumed structure length equal to the entire length of RAW (115 km), the percentage of rupture would be 13.5% ($\pm$ 5.8%). This corresponds to a rupture length of 16 km ($\pm$ 5.5 km).

A second estimate of rupture length is obtained by assuming that one-half of the longest mapped fault along RAW will rupture at the closest distance to RAW to the site. The maximum inferred length of the Wallula Gap fault is 45 km; a half-length rupture would be 23 km. This rupture is assumed to occur at the closest approach of faults along the RAW trend to the site (20 km), which would place the rupture segment along domain II. Because there is no evidence for a throughgoing fault along domain II, it is believed that a 23 km-long rupture within this domain is very unlikely.

The downdip fault width for a vertical strike-slip fault along RAW may be estimated from crustal models based on seismicity and geophysical data. A vertical fault that extends to the average maximum depth to basement, based on a time-term analysis (Eaton, 1976), would have a width of 7.5 km. A 12 km width is derived by extending a vertical fault to the depth above which nearly all of the instrumental seismicity occurs (Appendix 2.5J).

The following table summarizes the magnitude-related fault parameters for RAW assuming a strike-slip model:

Total Length	45 to 115 km
Rupture Length	16 to 23 km
Fault Width	7.5 to 12 km

Maximum Magnitude Relationships

Rupture Length vs. Magnitude (length in meters)

Strike-Slip: $M = 0.597 + 1.351 \log L$ (Slemmons, 1977)

Reverse-Oblique: $M = 4.398 + 0.568 \log L$ (Slemmons, 1977)

Area vs. Magnitude (area in square kilometers)

All fault types: $M = 4.15 + \log A$ (Wyss, 1979)

Magnitude Estimates

Based on the empirical relationships and the fault parameters presented above, maximum earthquake magnitudes are estimated and are presented below.

Reverse-Oblique-Slip Model:

Wallula Gap Fault

Technique	Maximum Magnitude
Rupture Length	6.9
Area	6.2 to 6.6
Estimate	6-1/2 to 7

Rattlesnake Mountain Fault

Technique	Maximum Magnitude
Rupture Length	6.5 to 6.7
Area	5.7 to 6.2
Estimate	6 to 6-1/2

Few data constrain the rupture length-magnitude relationship of Slemmons (1977) for $M < 7$ for reverse-oblique-slip faulting, and the correlation coefficient of this relationship is low (0.52). The area-magnitude relationship of Wyss (1979) is much better constrained at these magnitudes. Therefore, the maximum magnitude estimates based on fault area are preferred.

Strike Slip Model:

Rattlesnake-Wallula Alignment

Technique	Maximum Magnitude
Rupture Length	6.3 to 6.5
Area	6.2 to 6.6
Estimate	6-1/2

In summary, the estimates of maximum magnitude are given below:

Source	Tectonic Model	M max.	Distance to Site
Wallula Fault	Reverse-Oblique-Slip	6-1/2 to 7	42 km
Rattlesnake Mtn.	Reverse-Oblique-Slip	6 to 6-1/2	20 km
RAW	Strike-Slip	6 to 6-1/2	20 km

Ground Motions

Attachment A to Appendix 2.5K of Amendment No. 18 describes attenuation relationships that were used in the seismic exposure analysis of the WNP-2 and WNP-1/4 site. Data from the 1971 San Fernando, California earthquake, in which the type of faulting was reverse-oblique-slip, were used to define attenuation relationships for magnitude 6-1/2. The attenuation

relationships presented in Attachment A of Appendix 2.5K are reasonably applicable to the hypothesized events on RAW for which the type of faulting is reverse-oblique-slip.

Idriss, et al (1982) developed general attenuation relationships that incorporate data from strike-slip earthquakes as well as from earthquakes having other types of faulting. For the hypothesized strike-slip earthquake on RAW, it is judged that these relationships are more applicable than those in Attachment A of Appendix 2.5K.

Using the attenuation relationships referred to above, the following estimates of site peak ground acceleration are obtained for the hypothesized maximum earthquakes:

Source	Maximum Magnitude	Dist. (km)	Peak Ground Acceleration (g) Median	84th percntl
Wallula Fault (Reverse-Oblique-Slip)	6-1/2 to 7	42	0.08 to 0.11	0.11 to 0.16
Rattlesnake Mountain Fault (Reverse-Oblique-Slip)	6 to 6-1/2	20	0.14 to 0.18	0.20 to 0.26
RAW (Strike-Slip)	6-1/2	20	0.17	0.25

Note that for the magnitude 6-1/2 reverse-oblique-slip events in the above table, Equation 2.5K-A2 of Attachment A of Appendix 2.5K was used because it is the direct result of analysis of the data from the magnitude 6-1/2 San Fernando earthquake. For the magnitude 6 and 7 reverse-oblique-slip events in the above table, the generalized attenuation relationship given in Equation 2.5K-A6 was used.

Maximum magnitude estimates of 7 on the Wallula Gap fault and 6-1/2 on the Rattlesnake Mountain fault are judged to be less credible than the other estimates of maximum magnitudes presented above because of the lesser reliability of the length-magnitude correlation used to obtain these estimates, as discussed previously. Consequently, the best estimates for the peak ground accelerations range from 0.08 g to 0.17 g at the median level and 0.11 g to 0.25 g at the 84th percentile level.

Estimates of site response spectra have been made using the higher accelerations in the ranges cited above, 0.17 g (median) and 0.25 g (84th percentile). NUREG/CR-0098 (U.S. Nuclear Regulatory Commission, 1978) was used to estimate response spectra in two ways: 1) multiplying the median peak acceleration by the 84th percentile amplification factors given in NUREG/CR-0098, and 2) multiplying the 84th percentile peak acceleration by the median amplification factors given in NUREG/CR-0098. The resulting response spectra (damping ratio of 0.02) are compared in Figure 360.014-2 with the NRC Regulatory Guide 1.60 spectrum anchored to the SSE peak ground acceleration of 0.25 g. (The WNP-2 plant has been analyzed and found to be adequate for the Regulatory Guide 1.60 spectrum anchored to 0.25 g.) Figure 360.014-2 indicates that the derived site response spectra are lower than or equal to the Regulatory Guide 1.60 spectrum at all periods.

REFERENCES:

Bentley, R. D., Anderson, J. L., Campbell, N. P., and Swanson, D. A., 1980, Stratigraphy and Structure of the Yakima Indian Reservation, with Emphasis on the Columbia River Basalt Group: U.S. Geological Survey, Open-File Report 80-200, 83 p.

Cowan, D. S., 1981, The origin of the Umtanum Ridge-Gable Mountain structural trend and implications for a regional tectonic model: Appendix 2S to Skagit/Hanford Nuclear Plant Preliminary Safety Analysis Report, Prepared for Golder Associates, 21 p.

Eaton, J. P., 1976, Note on the Distribution of Earthquakes within and near the Hanford Seismic Network, 1969-1974, and Preliminary Results on Crustal Structure of the Region Obtained from an Analysis (by the Time-Term Model) of Industrial Explosions Recorded by the Network, Informal Notes: U.S. Geological Survey, Menlo Park, CA, 22 p.

Idriss, I. S., Sadigh, D., and Power, M. S., 1982, Variations of Peak Accelerations and Velocities with Magnitude to Close Distances to the Source, Paper prepared for presentation at April 1982 SSA Meeting.

Kendall, J. J., Dale, R. C., and Davis, G. A., 1981, The Structural Relationship of the Olympic-Wallula Lineament, Hite Fault System and LaGrande Fault System, the Blue Mountains of Umatilla County Oregon: Geological Society of America Abstracts with Programs, v. 13, no. 2, p. 64.

Myers, C. W., and Price, S. M., 1979, Geologic Studies of the Columbia Plateau: A Status Report: Rockwell-Hanford Operations, Richland, WA, RHO-BWI-ST-4.

Price, E. H., 1981, Structural Geometry, Strain Distribution and Tectonic Evolution of Umtanum Ridge at Priest Rapids and a Comparison with Other Selected Localities within Yakima Fold Structures, South-Central Washington: PhD Dissertation, Washington State University, 195 p.

Raisz, E., 1945, The Olympic-Wallowa Lineament: American Journal of Science, v. 243-A, p. 479-485.

Savage, J. C., Lisowski, M., and Prescott, W. H., 1981, Geodetic Strain Measurements in Washington: Journal of Geophysical Research, v. 86, no. B6, p. 4929-4940.

Shackleton, N. J. and Opdyke, N. D., 1973, Oxygen Isotope and paleomagnetic stratigraphy of Equational Pacific Core V28-238: Oxygen isotope temperatures and ice volumes on a 10^5 year and 10^6 year scale: Quarternary Research, v. 3, p. 39-55.

Slemmons, D. B., 1977, Appendix E to Safety Evaluation Report related to the operation of San Onofre Nuclear Generating Station Units 2 and 3: U.S. Nuclear Regulatory Commission, NUREG-0712, Docket Nos. 50-361 and 50-362, 28 p.

Slemmons, D. B., 1977, State-of-the-art for Assessing Earthquake Hazards in the United States, Report 6: Faults and Earthquake Magnitude: U.S. Army Corps of Engineers, Waterways Experiment Station, Soils and Pavements Laboratory, Vicksburg, MS, Miscellaneous Paper S-73-1, 129 p.

System, Science, and Software, 1980, Determination of Three-Dimensional Structures of Eastern Washington from the Joint Inversion of Gravity and Earthquake Travel Time Data: report prepared for Weston Geophysical Corporation by Rodi, W. L. et al., 143 p.

U.S. Nuclear Regulatory Commission (1978), Development of Criteria for Seismic Review of Selected Nuclear Power Plants, NUREG/CR-0098, by N. M. Newmark and W. J. Hall.

Woodward-Clyde Consultants, 1981, Wallula Fault Trenching and Mapping: Draft report prepared for Washington Public Power Supply System, Richland, WA.

Wyss, M., 1979, Estimating Maximum Expectable Magnitude of Earthquakes from Fault Dimensions: Geology, v. 7, no. 7, p. 336-340.

WASHINGTON PUBLIC POWER SUPPLY SYSTEM
Nuclear Project No. 2

MAP OF THE CLE ELUM–WALLULA LINEAMENT (CLEW)

Figure 360.14-1

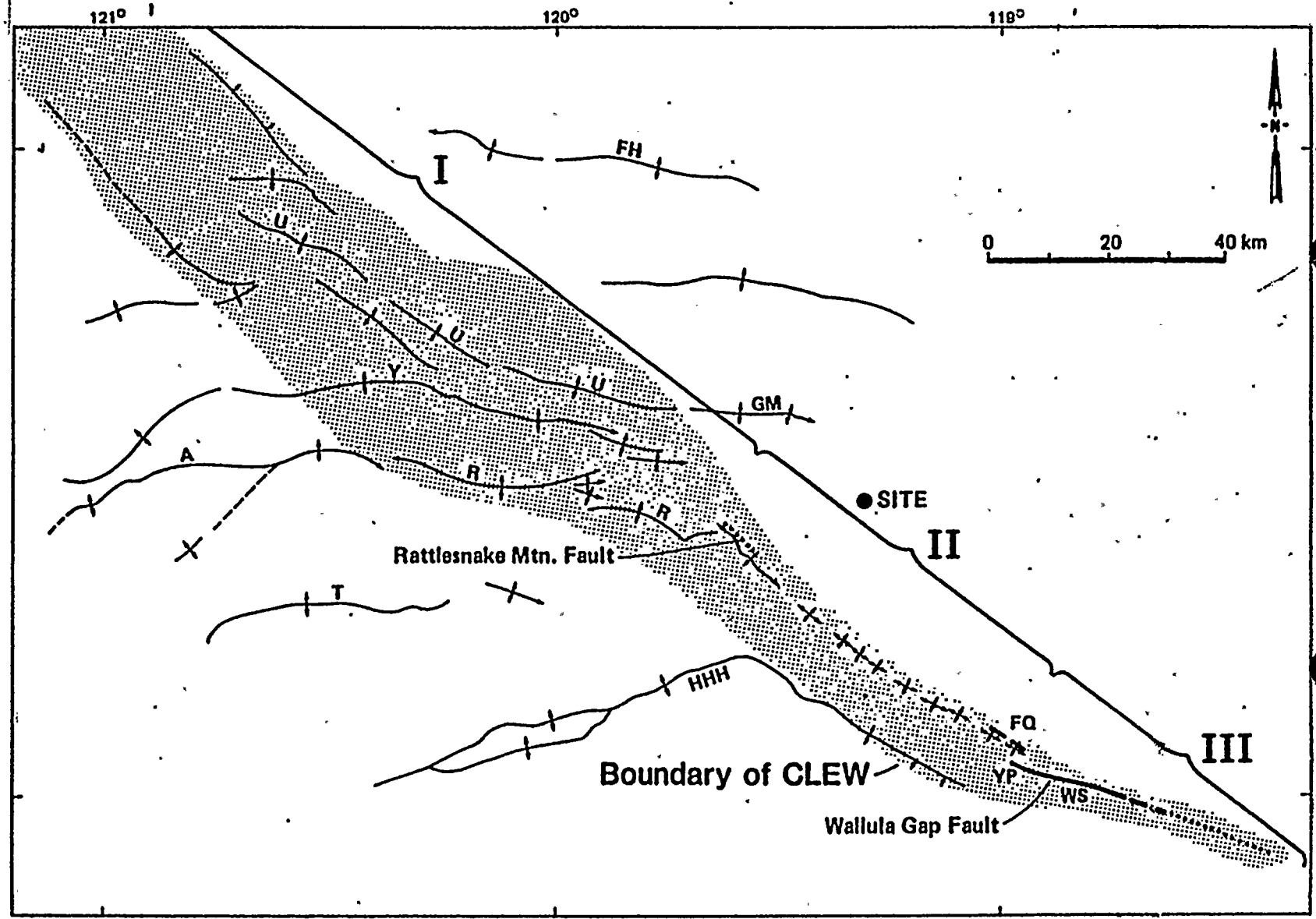

Map of the Cle Elum-Wallula Lineament (CLEW) showing structural domains I, II, and III. The Rattlesnake-Wallula alignment (RAW) is comprised of domains II and III. Names of anticlinal ridges are: A, Ahtanum Ridge; FH, Frenchman Hills; GM, Gable Mountain; HHH, Horse Heaven Hills; R, Rattlesnake Hills; SM, Saddle Mountains; T, Toppenish Ridge; U, Umtanum Ridge; Y, Yakima Ridge. Localities along RAW are: FQ, Finley Quarry; YP, Yellepit; WS, Warm Springs.

WASHINGTON PUBLIC POWER SUPPLY SYSTEM
Nuclear Project No. 2

COMPARISON OF SITE RESPONSE SPECTRA OBTAINED USING NUREG–CR 0098 WITH REGULATORY GUIDE 1.60 RESPONSE SPECTRUM

Figure 360.14-2

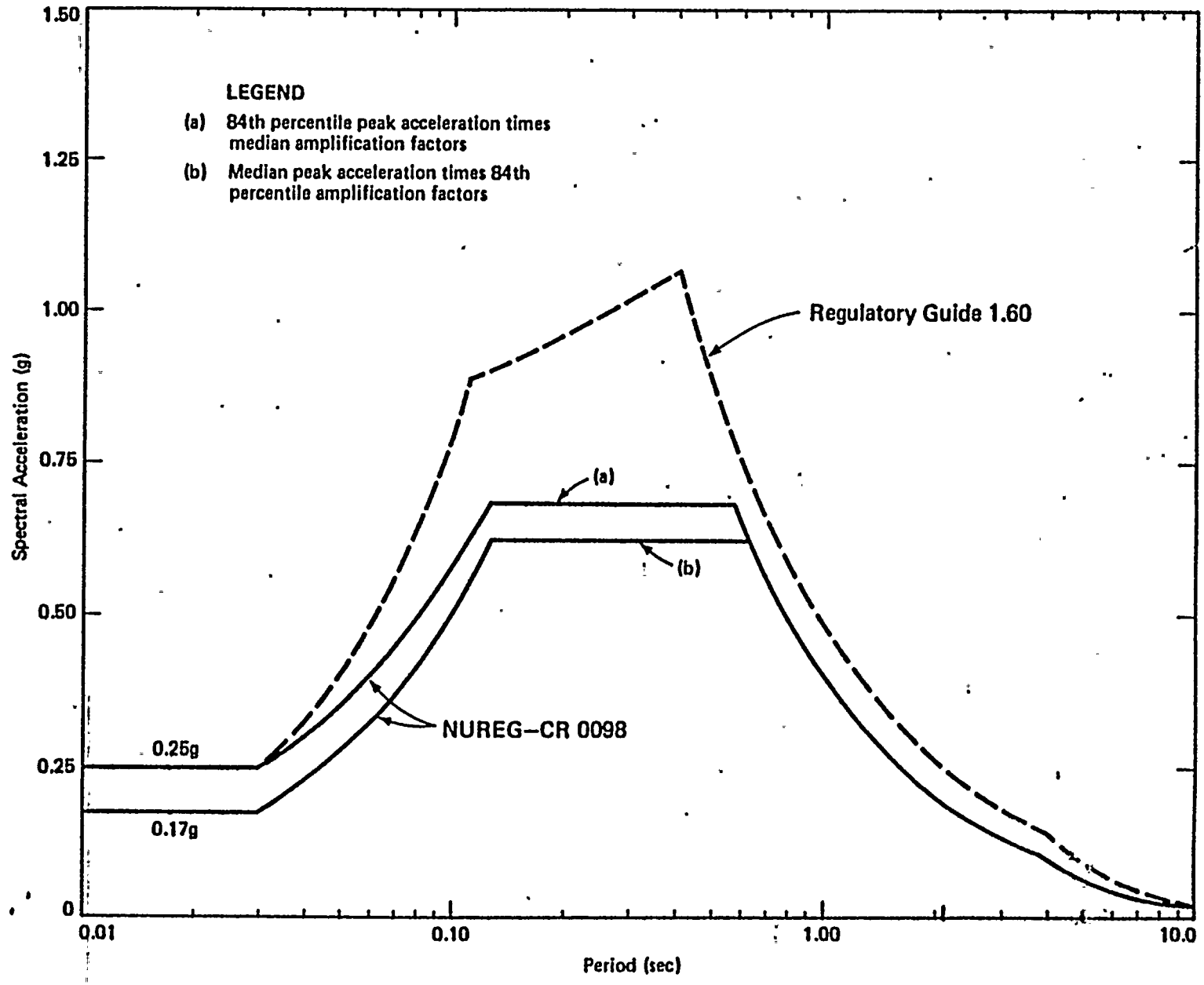

360.17

In the section on Umtanum Ridge - Gable Mountain, reference was made to the Golder report to NESCO. Reevaluate the structural and/or tectonic model on Umtanum Ridge in light of the geologic map and cross section of the Golder report (Figure 2N-11, 2N-13) suggesting normal faulting on Umtanum where reverse arrows are shown. (Contact Tim Hait, USGS.)

RESPONSE

In this response, cross section A-A' (Golder, 1981; Figure 2N-13) is reevaluated in light of three possible models to explain the anomalous apparently normal displacement on the Umtanum fault and local structural complexities in the Filey Road area (Figure 1).

The Umtanum fault is clearly a reverse fault along which distinctly older units have been thrust over younger basalt flows in a compressional stress regime (Golder, 1981; Figure 2N-11). This style of faulting is observed over all but 1 1/2 miles of the inferred length of 19 miles for this fault along the northern margin of the eastern segment of Umtanum Ridge. An apparent anomaly in this dominantly older-over-younger relationship exists along two short segments of the fault trend where lithology and structure are particularly complex. In cross section A-A' (Golder, 1981; Figure 2N-13) stratigraphic units are juxtaposed across the Umtanum fault with an apparent normal sense of displacement rather than the reverse sense of displacement, which is indicated by arrows on this figure and typical of the fault.

The geologic structure from the Yakima Firing Center boundary to 1/2 mile west of cross section A-A' on Figure 2N-11

(Golder, 1981) is considerably more complex than in adjacent areas near Priest Rapids Dam (on the east) and Sourdough Canyon (on the west). This intervening area is characterized by apparently repeated east-west trending bands of Grande Ronde, Vantage, Frenchman Springs, and Roza Members lying north of the mapped trace of the Umtanum fault on Figure 2N-11. These bands of rock and associated structural complexities are not known to be present elsewhere along the northern margin of this ridge segment. Thus, geologic conditions here appear to reflect unique, local structural relationships that exist only along this 1 1/2 mile section of the ridge front.

General

Before discussing the four models, several observations can be made concerning the geology shown on Figure 2N-11 (Golder, 1981). This figure is reproduced here as Figure 1 with certain modifications (described in the following sections) which have been made on the basis of a reevaluation of cross section A-A'. Figure 1 should be used with reference to the following points.

1. The area of complex structure underlain by older Wanapum and Grande Ronde Basalt units forms a lobate mass that lies north of the Umtanum fault and extends only 1 1/2 miles east-west from near Filey Road to just west of section line A-A'.

2. South of the mapped trace of the Umtanum fault, basalt units in the hanging wall trend east-west and are uniformly steeply dipping and overturned from east of Priest Rapids Dam to Sourdough Canyon along the entire northern ridge front.

3. Units within the lobate mass lying between the Umtanum fault and the possible reverse fault along section A-A' dip to the south or north at 20° or less and are not overturned. Units between the possible reverse fault and the north reverse fault dip approximately 15° to 20° south and are not overturned.

4. The footwall exposures between Priest Rapids Dam and Sourdough Canyon are primarily gently north-dipping basalt flows of the Priest Rapids Member which is structurally very little disturbed. A gentle anticlinal warp in footwall rocks is present just to the north of the north reverse fault.

5. The presence of gently dipping Priest Rapids Basalt in the footwall east, north, and west of the lobate mass of upright older Wanapum and Grande Ronde rocks indicates that these complexly deformed units must be bounded by a subhorizontal fault along their western margin (not previously shown on Figure 2N-11 but included on Figure 1 here) which connects the western end of the north reverse fault to the main Umtanum fault along a northeast-southwest trend.

6. The area along the Umtanum fault trace where younger rocks (Frenchman Springs Member) are mapped as being anomalously thrust over older units (Grande Ronde Basalt) extends for less than 1 mile along the fault trace on either side of section A-A' (Golder Associates, 1981; Figure 2N-11). Roza Member is also shown as being thrust over Grande Ronde Basalt along a short section of the Umtanum fault trace 1/2 mile east of Filey Road. Along the remainder of the Umtanum fault trace from east

of Priest Rapids Dam to west of Sourdough Canyon (a distance of approximately 19 miles), hanging-wall rocks of the same age as, or distinctly older than, footwall rocks are thrust northward over the footwall. Thus, the anomalous normal displacement suggested by the presence of younger units juxtaposed over older units occurs only along a very short section of the mapped trace of the Umtanum fault.

Models

Although field evidence clearly demonstrates reverse movement on the Umtanum fault, several possible explanations for local geologic conditions suggesting normal displacement are presented in the following three models. Cross section A-A' (Golder, 1981; Figure 2N-13) is reproduced here as Figure 2 with only the attitudes of the various units shown. Faults are not shown on this structural representation. The three models describe mechanisms which might have produced the pattern and attitudes of rock units shown on this section and on the geologic map (Figure 1). The first two models (imbricate thrusting in a double fold and landsliding) are considered the most reasonable explanations of the anomalous relationships; these two models are in agreement with the observations made in the previous section. The third model (antithetic faulting in the hanging wall of imbricate reverse faulting) is incompatible with the field relationships described in the previous section.

Model 1: Imbricate Thrusting in a Double Fold

In this model (Figure 4), a small subsidiary fold is inferred to have formed in front of (north of) the main Umtanum fold in the Filey Road area and to have extended from the Yakima

Firing Center boundary to 1/2 mile west of cross section A-A'. The axis of this subsidiary fold was convex to the north (Figure 4A).

As folding proceeded, reverse faulting, which was elsewhere confined to the northern base of the main Umtanum Ridge anticline, first occurred near the northern margin of the subsidiary fold in the Filey Road area (Figure 3B), displacing a south-dipping sequence of older Wanapum Basalt units over basalt flows of the Priest Rapids Member along the north reverse fault. In this initial phase of folding and generation of a thrust fault from the core of the main anticline, the area of maximum shortening along the syncline axis near Filey Road was elevated with respect to the general structural position of the syncline along the major portion of the main fold front on the northern flank of the ridge (Figure 3). This local upwarping of the syncline axis is attributed to the presence of the subsidiary anticline north of the main fold in the Filey Road area. As a consequence, the thrust fault (Umtanum fault), which propagated from the core of the main concentric fold structure, locally intersected the ground surface north of the axis of maximum shortening along the ridge front in the Filey road area (Figure 3A and 3B) during this initial stage of fold/fault development.

In a subsequent phase of the folding process (Figure 4A), thrust faulting occurred along the possible reverse fault, and the north reverse fault became inactive. During this second phase of faulting, Frenchman Springs and Grande Ronde basalt flows were thrust over Priest Rapids and Frenchman Springs basalt flows.

In a third phase of folding (Figure 4B), faulting again stepped to the south, and Grande Ronde Basalt was thrust over basalt of the Frenchman Springs Member along a fault that had not been previously inferred on Figure 2N-11 (see Figure 1). Note that: (1) all three of these imbricate thrust wedges involve rocks present in the subsidiary fold just north of the main Umtanum Ridge anticline and (2) these units are not overturned.

This southward migration of imbricate thrusting in the Filey Road area reflects local, near-surface adjustments in the position of the fault plane as it migrated toward the adjacent syncline which marked the axis of maximum shortening south of the subsidiary fold. Elsewhere along the ridge, this syncline was already the locus of the intersection of faulting with the ground surface (Figure 3A and 3B). Thus, a stepwise migration of faulting to the zone of maximum shortening along the syncline axis occurred locally during later stages of growth of the main fold in the Filey Road area.

As faulting occurred along these local imbricate thrusts, folding and overturning of basalt units in the main anticline proceeded until, finally, thrust faulting also occurred in the Filey Road area at the base of the main anticline where maximum shortening was occurring throughout the eastern segment of Umtanum Ridge (Figure 4C). Because basalt flows of the Frenchman Springs Member were already sharply folded and overturned in the main anticline, thrusting along the Umtanum fault in this area (as shown on Figure 1) resulted in the juxtaposition of younger (Frenchman Springs) basalt over older (Grande Ronde) basalt (Figure 5), a situation made possible by the prior uplift and thrusting of these older units in the local, subsidiary anticline.

Thus, the final step in this model shows a cross-sectional pattern compatible with that observed in Figure 2 and on the geologic map (Figure 1). The faulting is inferred to be a product of folding of a concentric fold in a compressional stress regime, and the anomalous local juxtaposition of younger rocks over older rocks is explained by the presence of a small, subsidiary anticline to the north of the main Umtanum fault. The south-stepping activity on faults is supported by the observation that the most northerly fault in the area, the north reverse fault, is overlain by undisturbed basalt of the Pomona Member at an elevation of approximately 800 to 850 feet above sea level. These relationships demonstrate inactivity on this fault for the last 12 m.y. However, the presence of basalt of the Pomona Member on the southern flank of Umtanum Ridge at an elevation of 2030 feet indicates that folding and faulting continued in post-Pomona time along the main part of the ridge. This model is also compatible with: (1) the distribution of east-west trending rock belts formed by the imbricate thrust slices, (2) the observed basalt flow attitudes, (3) the localization of the main Umtanum fault at the northern margin of tightly folded and overturned Wanapum units, (4) the apparent shallow dips of thrust faults in the area as inferred from map patterns, and (5) the lobate shape of upright hanging-wall rocks that lie north of the more tightly folded overturned units forming the northern margin of the anticline elsewhere along the northern limb of the main fold.

Model 2: Landsliding

Another model involves northward sliding of very large landslide blocks off the uplifted crest of Umtanum Ridge fold (Figures 6 and 7). In this model, the most northerly fault (the north reverse fault) is at the toe of the large, lobate rock mass

of older Wanapum and Grande Ronde Basalt which is interpreted as a landslide complex in this model. Figure 8 is a sketch of the structural configuration of the eastern segment of Umtanum Ridge between Sourdough Canyon and Priest Rapids Dam. The Twin fault is considered to be a tear fault across which differential folding of the ridge front occurred. Units to the west of this fault are more tightly folded and overturned than units to the east. The upper reverse fault is a low angle thrust in the hinge area of the fold where units in the upper limb overrode units in the steeply dipping northern limb. The upper reverse fault resembles the Buck thrust of Price (1981a) in this respect. Periodic oversteepening of the fold and associated landsliding could account for the complex lobate rock mass which now lies to the north of what is shown as the Umtanum fault on Figure 1.

As sliding proceeded, progressively deeper portions of the fold hinge and older rocks were exposed. As a result, the roughly arcuate slide masses are now stratigraphically reversed, with older rocks overriding younger rocks in a pattern resembling imbricate thrusting (Figure 6B and 6C). The oldest sliding event is considered to be pre-Pomona in age (12 m.y.) beause undisturbed basalt of the Pomona Member overlies the northern margin of the inferred slide mass. Subsequent episodes of folding again oversteepened the north flank of the ridge in the area of the upper reverse fault and resulted in further sliding of large blocks off the crest. Movement along the Umtanum fault later juxtaposed overturned younger rocks (Frenchman Springs) in the hanging-wall over older rocks (Grande Ronde) in the youngest, most southerly slide mass lying on the subhorizontal footwall units (Priest Rapids) (Figure 7).

Thus, this model explains the apparent local juxtaposition of younger units over older units along the main Umtanum thrust.

The model is also in agreement with the general observations made in the first section of this response. The model does require significant pre-Pomona elevation of the Umtanum Ridge anticline to account for the massive landslides. That such relief existed is suggested by the presence of Pomona outcrops underlain by a basalt fanglomerate that is inferred to have been shed from the northern margin of Umtanum Ridge. The presence of this fanglomerate and its pre-Pomona age suggest that the anticline may have had sufficient relief to generate large landslides prior to 12 m.y. ago. The model does not explain why the localized oversteepening occurred west of the twin fault or how steeply dipping units on the ridge crest rotated to an upright position with subhorizontal to southerly dips which they now generally have in the hypothesized slide complex.

Model 3: Antithetic Faulting

A third model assumes that high-angle antithetic normal or reverse faulting occurred along what is mapped as the trace of the main Umtanum fault in the area between Filey Road and cross section A-A' on Figure 1. In this model, reverse displacement at the northern base of Umtanum Ridge is locally distributed over several imbricate thrust slices, the possible reverse fault and north reverse fault being the two most prominent structures along which reverse movement had occurred (Figure 9B to 9D). The Umtanum fault, which is considered an antithetic fault in the hanging wall of this thrust complex, displaces basalt of the Frenchman Springs Member against Grande Ronde Basalt with either a normal (Figure 9E) or reverse (Figure 9F) sense of offset.

Although both antithetic normal and antithetic reverse faulting have been observed in the hanging walls of thrusts, several problems exist in interpreting the Umtanumn fault as.

either one of these types of structures for the central part of the mapped area shown on Figure 1:

1. At all other locations along the northern margin of the eastern segment of Umtanum Ridge (including the Sourdough Canyon area immediately west and the Priest Rapids area immediately east) the Umtanum fault occurs at the base of the overturned, steeply-dipping hanging-wall rocks. In the Filey Road area, this structural position would be anomalously occupied by a normal fault or a north-dipping reverse fault.

2. Unlike rocks in the hanging wall elsewhere along the Umtanum fault, rocks in the imbricate thrust slices, which would have to accommodate the primary reverse displacement through this area, are not overturned. They are upright and generally dip at angles of less than 20 degrees. Thus, structural relationships in the hanging wall in the Filey Road area would be drastically different than those observed elsewhere along the northern margin of this ridge segment.

3. In the Filey Road area normal faulting or north-dipping reverse faulting along the presently mapped trace of the Umtanum fault would be in alignment with low-angle reverse faulting mapped immediately west in the Sourdough Canyon area (Figure 1) where good exposures exist. There is no indication of normal or antithetic reverse faulting along the trace of the Umtanum fault in the Sourdough Canyon area. The proposed antithetic faulting would have to terminate just west of cross section line A-A' on Figure 1 and not continue beyond the landslide complex at the eastern margin of the mapped area shown on Figure 1.

Thus, the inferred local antithetic normal or reverse displacement suggested by this model for the Umtanum fault does not fit observed structural relationships along the northern margin of Umtanum Ridge. The location of steeply dipping to overturned rock units along the northern flank of the ridge and the location of the hinge line of the anticline indicate that antithetic faulting should occur farther south in the hanging-wall sequence, not at the margin of overturning in the area of maximum shortening.

Discussion

None of the three possible models discussed here requires a reinterpretation of the fold/fault relationships presented in Golder (1981) to explain the local complex geologic structure and apparent normal faulting in the Filey Road area. The first two models are compatible with the general and specific field observations discussed in the report (Golder, 1981) on the eastern segment of Umtanum Ridge. The first model is compatible with faulting produced by folding in a north-south compressional stress regime and with imbricate thrusting produced locally in the Filey Road area by faulting of a small subsidiary anticline that developed just north of the main Umtanum anticline. In this model, reverse faulting occurred at the same time all along the northern margin of the ridge and was distributed over three or more imbricate thrust slices in this area, with the faulting stepping progressively to the south as the main anticline developed. In the final stage of development (Figure 4C), very tight folding and overturning of basalt flows in the main fold resulted in thrusting of younger units (Frenchman Springs) over older units (Grande Ronde) which had previously been uplifted and thrust northward in the small subsidiary fold (Figure 4A and 4B).

In the second model, landsliding accounts for the apparently anomalous displacement of younger units over older units on a reverse fault (Figures 5 and 6). The Umtanum fault remains a relatively simple structure compatible with its mapped expression to the east and west of the Filey Road area. The possible reverse fault and north reverse fault are interpreted as slide planes separating large individual slide masses. This model requires significant pre-Pomona uplift of the ridge to account for the movement of the first large body of rock from the ridge crest.

The third model places the principal thrusting associated with folding on the north reverse fault and possible reverse fault in the Filey Road area. As shown on the geologic map (Figure 1), the Umtanum fault is interpreted as a normal or reverse antithetic fault in the hanging wall of these imbricate thrust slices (Figures 10A and 10B). However, an antithetic fault in this location is incompatible with the observed structural relationships along the northern margin of Umtanum Ridge.

REFERENCES:

Golder Associates, 1981, Geologic structure of Umtanum Ridge: Priest Rapids Dam to Sourdough Canyon; Appendix 2N: Northwest Energy Services Company, Kirkland, Washington, 59 p.

Price, E.H., 1981a, Structural geometry, strain distribution and mechanical evolution of eastern Umtanum Ridge, and a comparison with other selected localities within Yakima fold structures, south-central Washington: Rockwell Hanford Operations, Richland, Washington, RHO-BWI-SA-138, 99 p.

Price, E.H., 1981b, Personal communication of sketch drawing to Golder Associates, December 8, 1981, Richland, Washington.

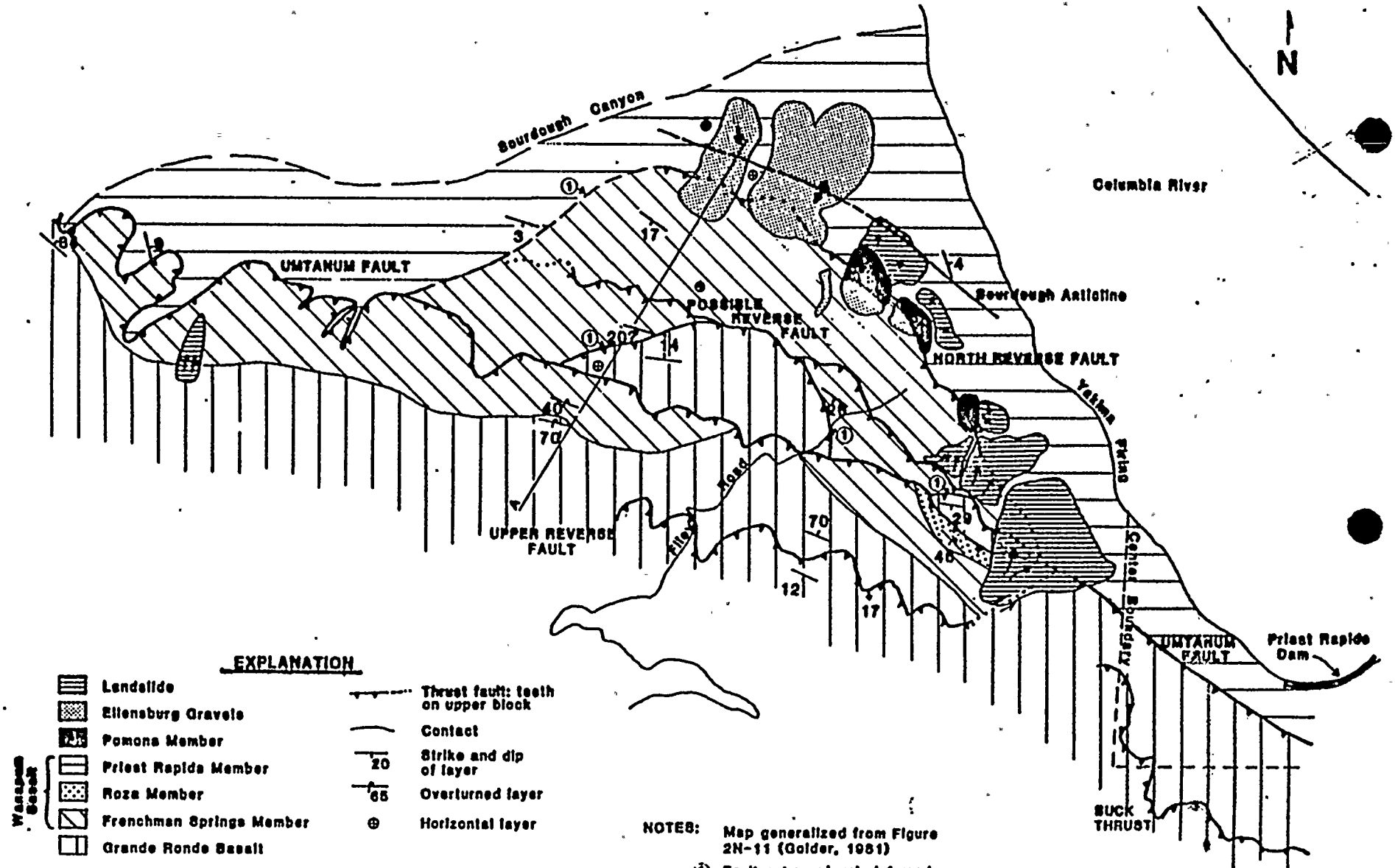

NOTES: Map generalized from Figure 2N-11 (Golder, 1981)

① Fault not previously inferred on Figure 2N-11 (Golder, 1981)

GENERALIZED GEOLOGIC MAP FIGURE 1

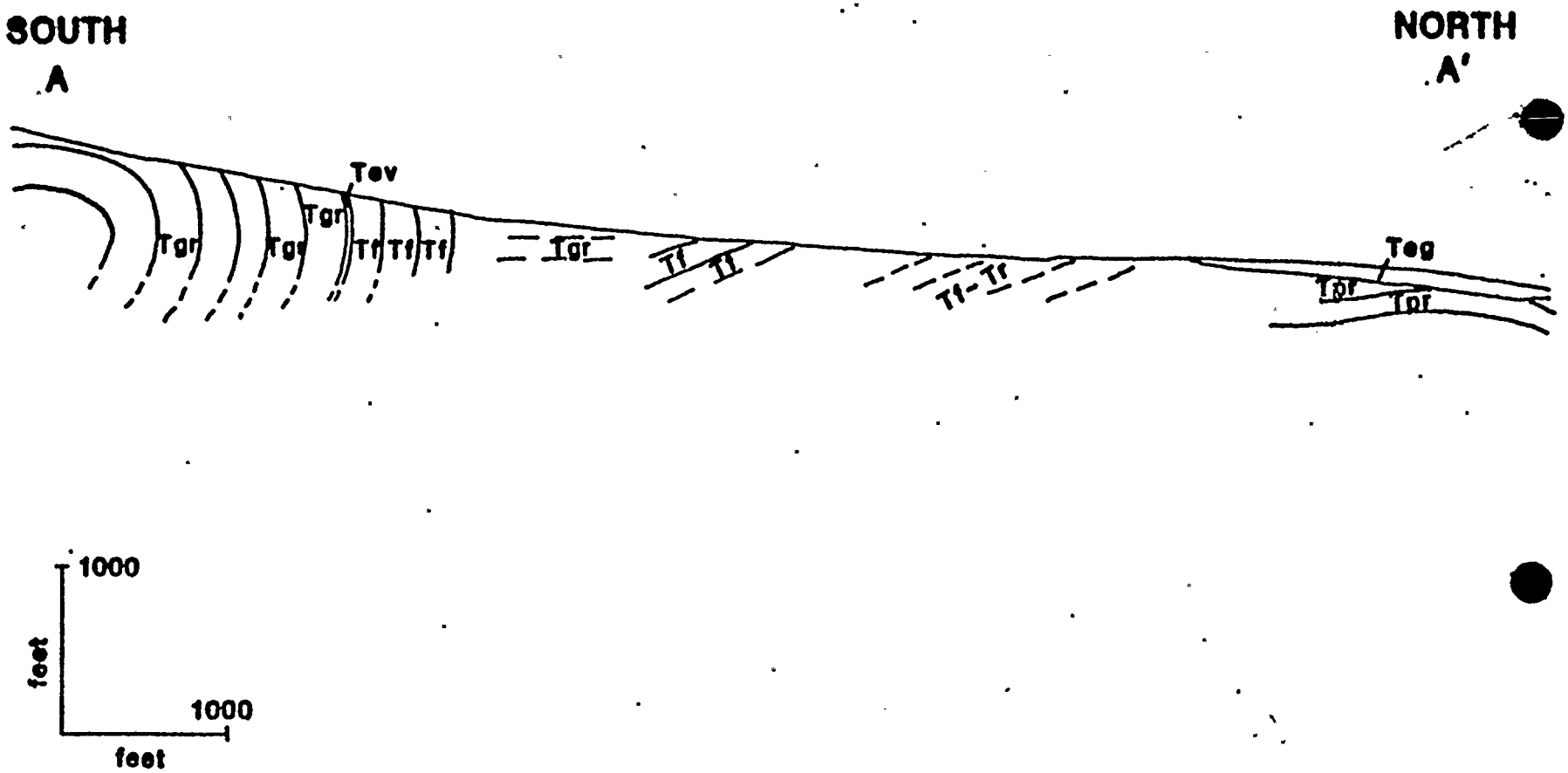
SOUTH
A
NORTH
A'
Tev
Tgr
Tgr
Tgr
Tf
Tf
Tf
Tgr
Tf
Tf
Tf
Tf
Tgg
Tgr
Tgr
1000
feet
1000
feet

FIGURE 2

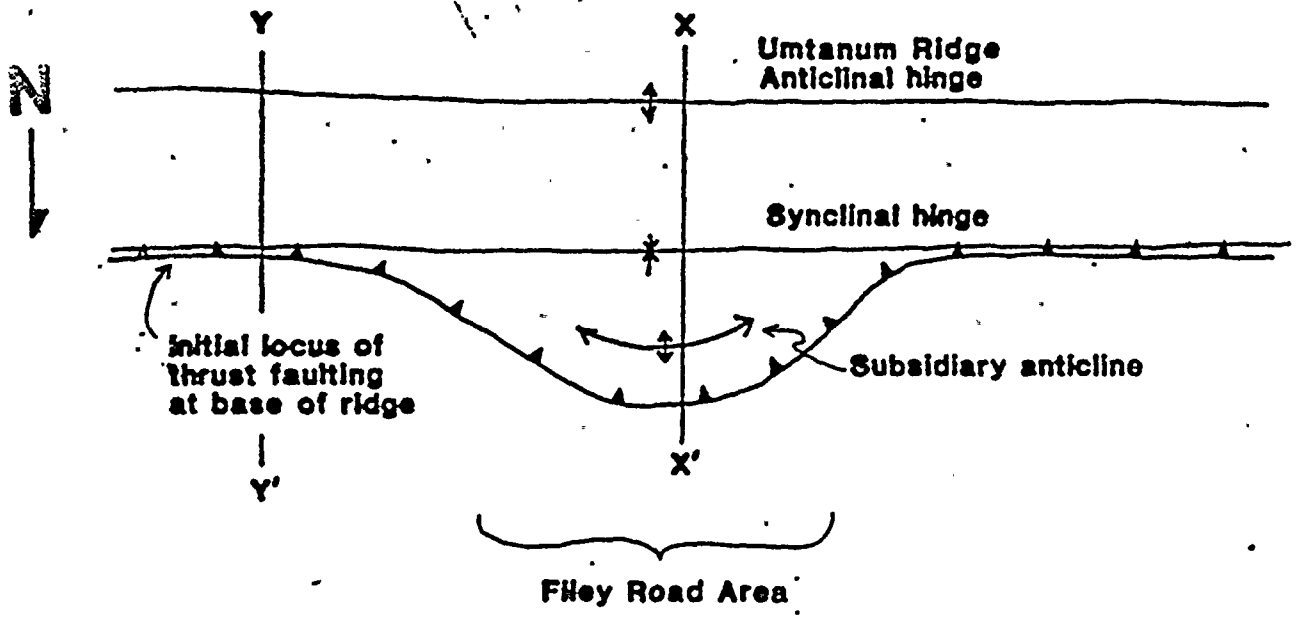

A. Plan view of main anticlinal trend and subsidiary anticline

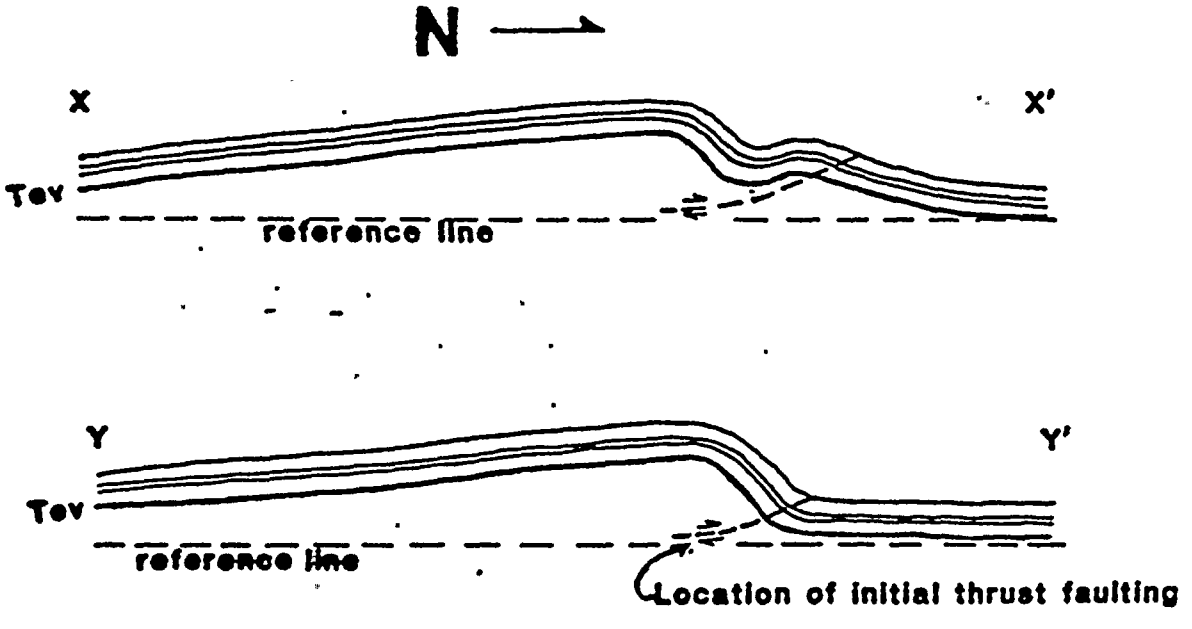

B. Generalized cross section(s) of Umtanum Ridge showing structural elevation of syncline axis in the Filey Road area (X–X') relative to adjacent areas (Y–Y')

FIGURE 3

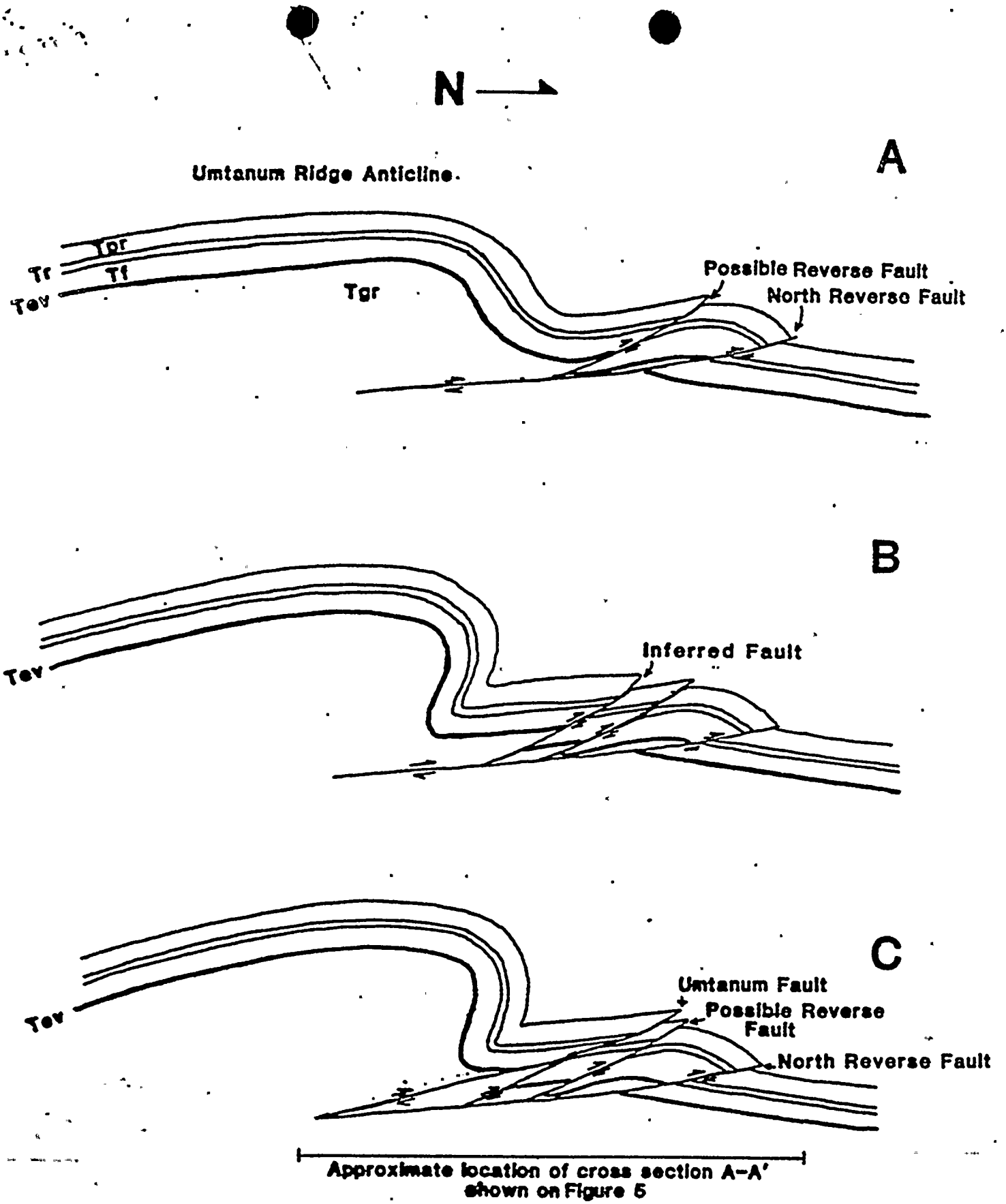

MODEL 1
IMBRICATE THRUSTING IN A DOUBLE FOLD

FIGURE 4

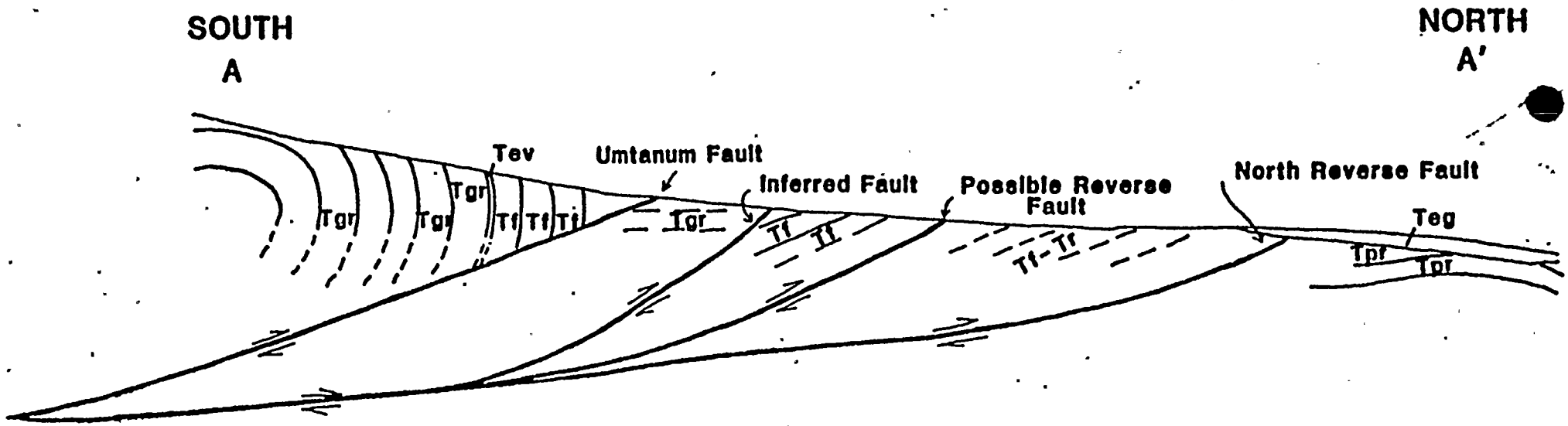
SOUTH
A
NORTH
A'
Tev
Umtanum Fault
Inferred Fault
Possible Reverse Fault
North Reverse Fault
Tgr
Tgr
Tgr
Tf
Tf
Tf
Tgr
Tf
Tf
Tf-Tr
Teg
Tpr
Tpr

FIGURE 5

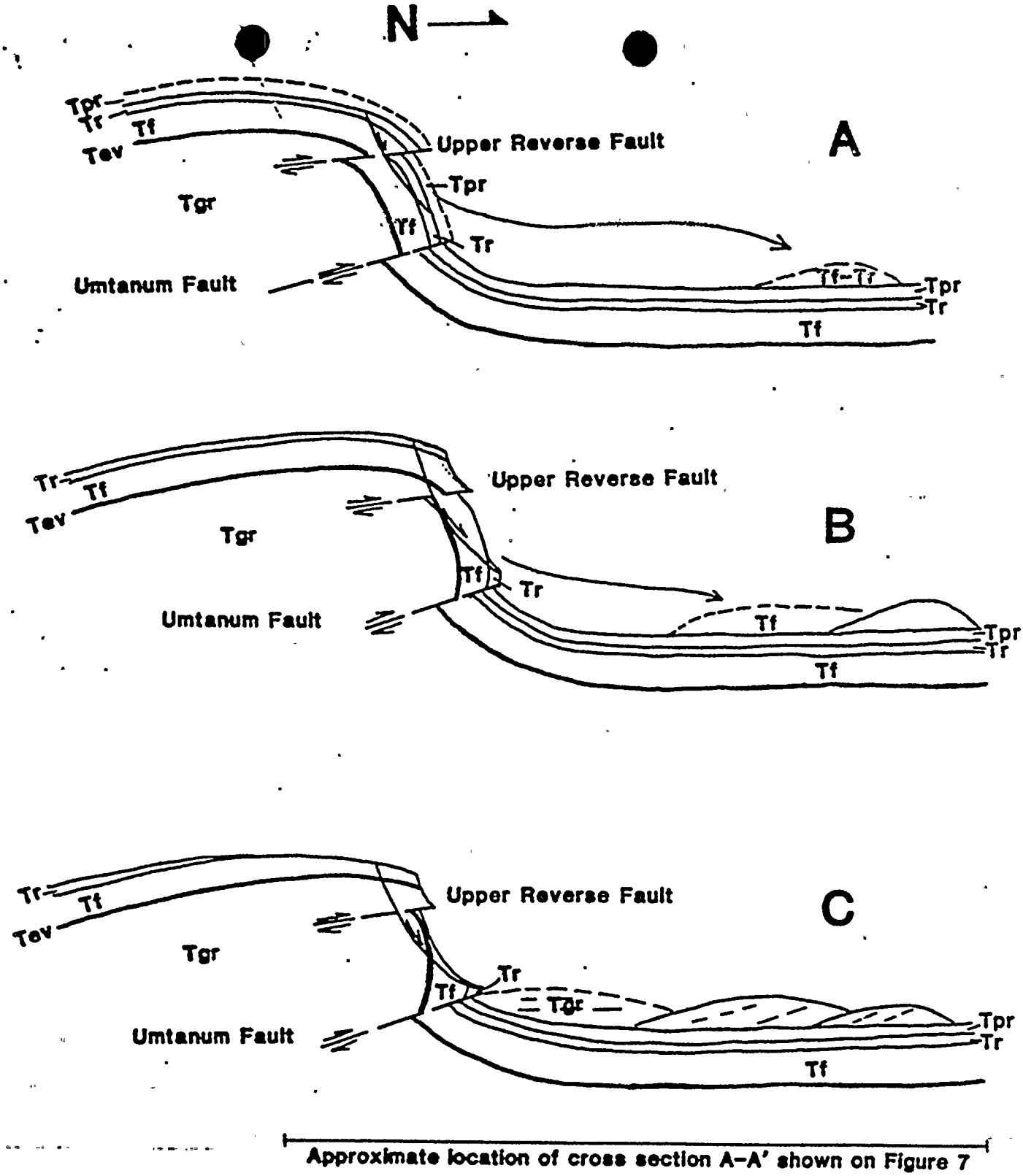

Approximate location of cross section A–A' shown on Figure 7

MODEL 2
LANDSLIDING

FIGURE 6

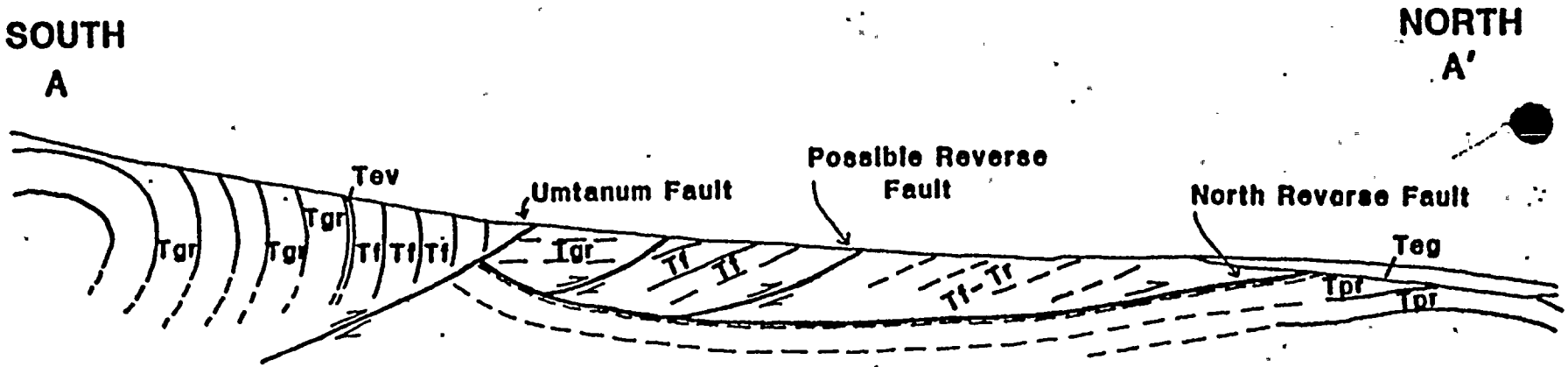
SOUTH
A
NORTH
A'
Tev
Tgr
Tgr
Tgr
Tf
Tf
Tf
Umtanum Fault
Igr
Possible Reverse
Fault
Tf
Tf
Tf-Tr
North Reverse Fault
Teg
Tpr
Tpr

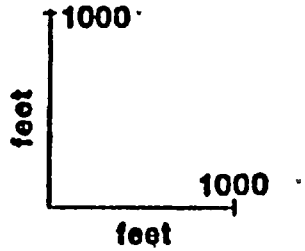
1000
feet
1000
feet

FIGURE 7

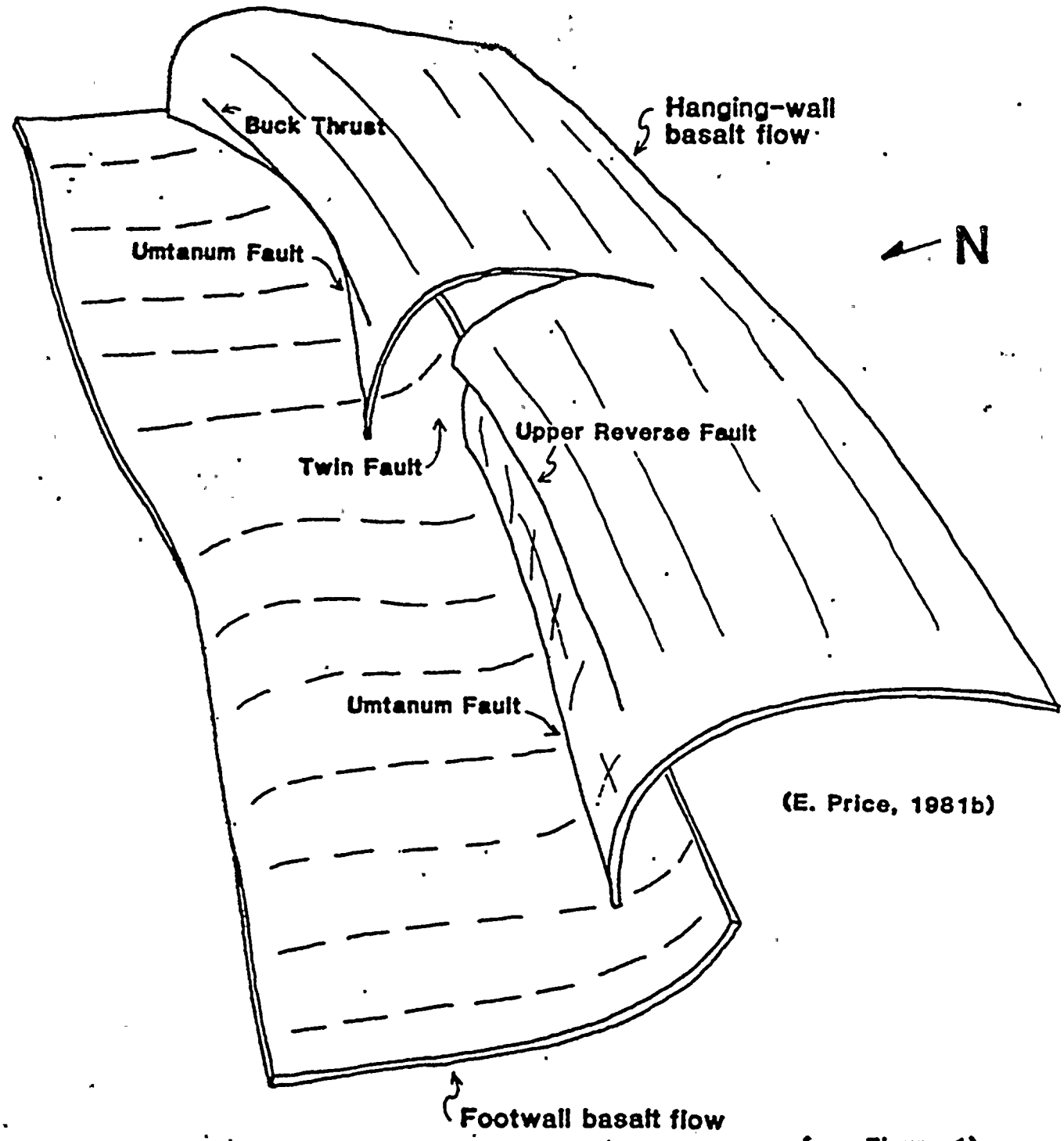

SKETCH OF UMTANUM-RIDGE STRUCTURE
IN FILEY ROAD AREA

FIGURE 8

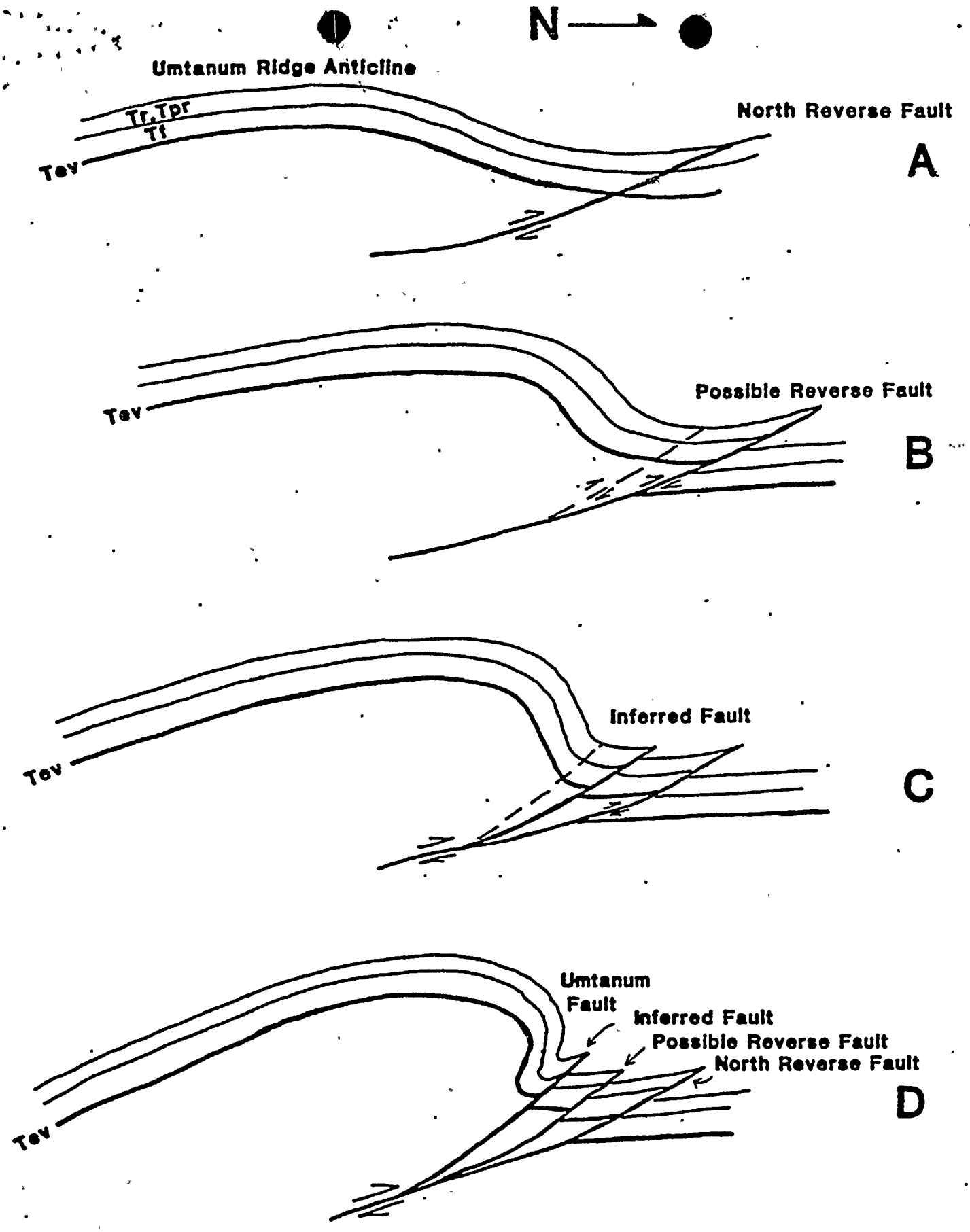

MODEL 3
ANTITHETIC FOLDING

FIGURE 9
Page 1 of 2

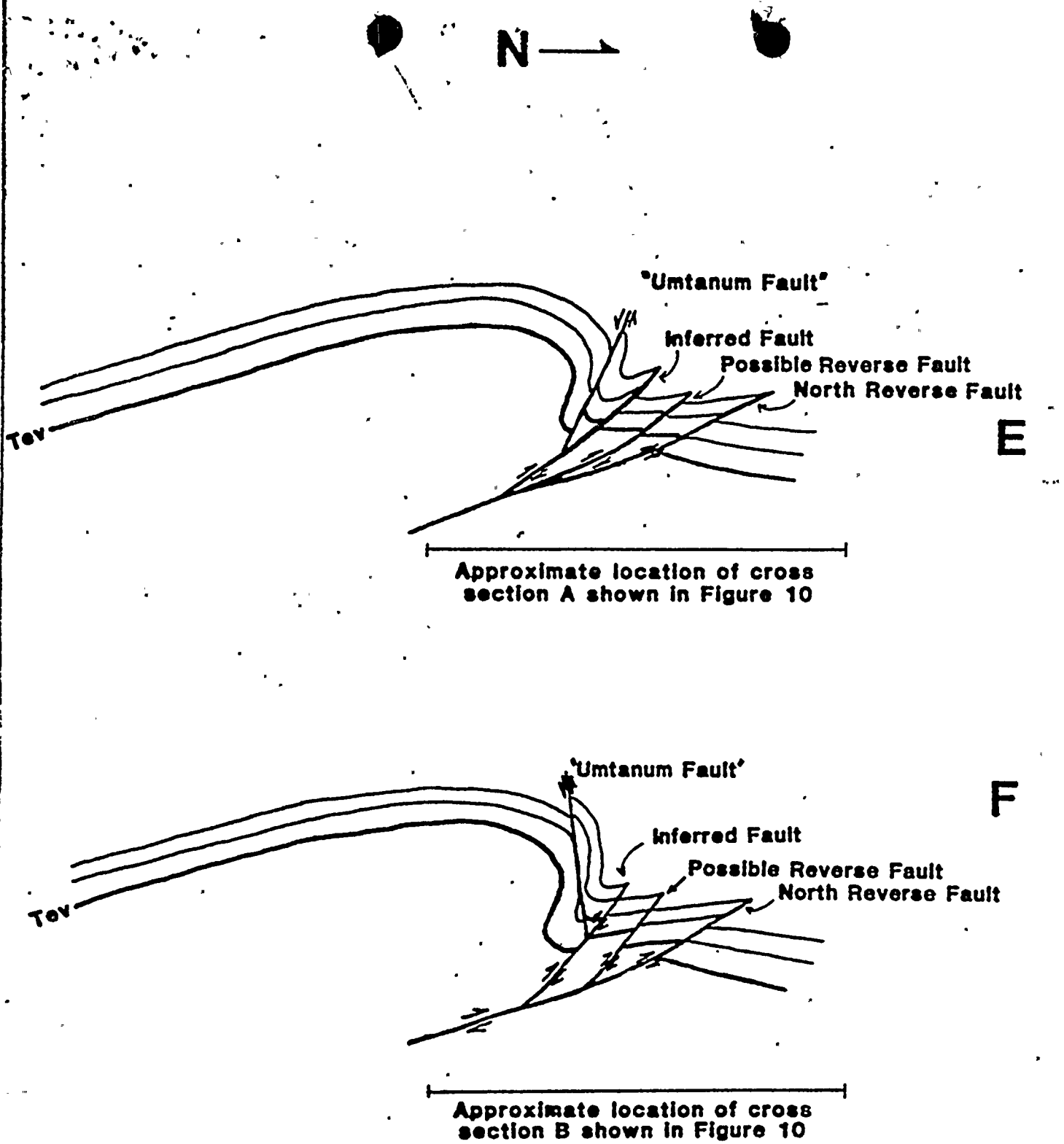

FIGURE 9
Page 2 of 2

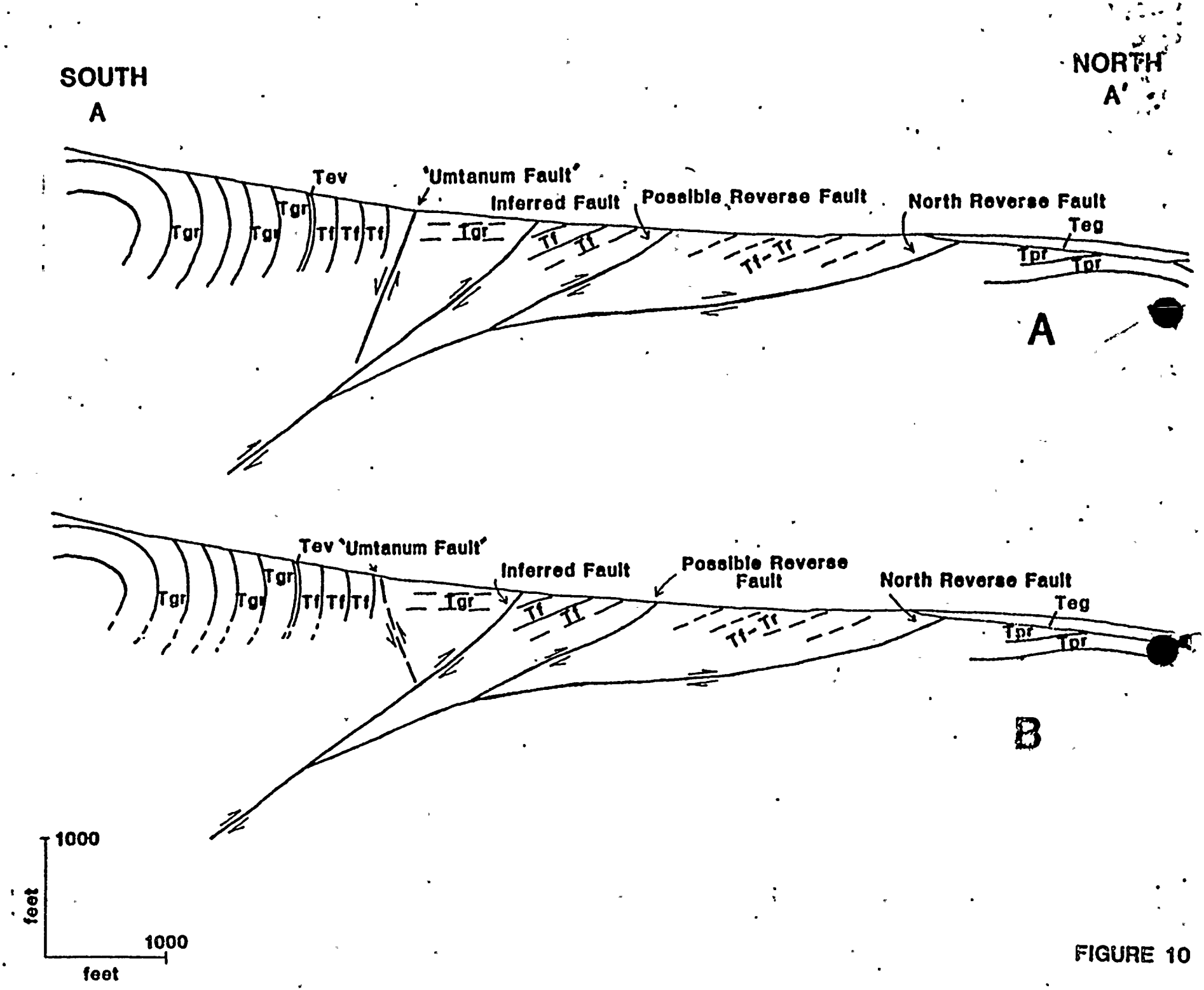
SOUTH
A
NORTH
A'
Tev
'Umtanum Fault'
Inferred Fault
Possible Reverse Fault
North Reverse Fault
Teg
Tpr
Tgr
Tf
Tf-Tr
Igr
A
Tev
'Umtanum Fault'
Inferred Fault
Possible Reverse Fault
North Reverse Fault
Teg
Tpr
Tgr
Tf
Tf-Tr
Igr
B
1000
feet
1000
feet

FIGURE 10